

# Ge redistribution in solid-phase Ge/Pd/GaAs ohmic contact formation

C. J. Palmström, S. A. Schwarz, E. Yablonovitch, J. P. Harbison, C. L. Schwartz,  
L. T. Florez, and T. J. Gmitter  
*Bellcore, Red Bank, New Jersey 07701-7040*

E. D. Marshall and S. S. Lau  
*Department of Electrical and Computer Engineering, University of California-San Diego,  
La Jolla, California 92093*

(Received 23 January 1989; accepted for publication 6 September 1989)

A backside secondary ion mass spectrometry technique is employed to examine elemental redistribution in the Ge/Pd/GaAs ohmic contact as a function of annealing conditions. Dilute Al containing marker layers ( $\text{Ga}_{1-x}\text{Al}_x\text{As}$ ) in the GaAs permit precise calibration and alignment of the elemental depth profiles. Double etch-stop thinning yields high depth resolution. The onset of ohmic behavior is found to occur when Ge is detected at the GaAs surface. Good ohmic behavior is observed when an interfacial layer of reacted  $\text{Pd}_3\text{GaAs}$  is dispersed and complete coverage of Ge occurs. The Ge/GaAs interface is abrupt with the Ge concentration dropping by over three orders of magnitude within 100 Å. About 40 Å of GaAs is found to be consumed during the ohmic contact formation. Degradation of the ohmic contacts, as a result of further heat treatment, was found to correlate with Ge in-diffusion into the GaAs. The results place strict limitations on doping and heterointerface models of ohmic behavior for this contact.

## I. INTRODUCTION

Ohmic contact formation to GaAs has been studied extensively,<sup>1-6</sup> yet the detailed mechanisms causing ohmic behavior are still debated for all practical contacts. The ubiquitous Au-Ge-Ni alloyed ohmic contact has been extensively studied since 1967,<sup>7</sup> but remains controversial.<sup>1</sup> A popular explanation for its ohmic behavior is that, during alloying of the contact, some GaAs is dissolved into the melt which, upon cooling, is rejected and regrows epitaxially on GaAs. Some Ge is incorporated into this regrown layer and dopes the GaAs sufficiently *n* type<sup>8</sup> to permit electron tunneling to dominate at the contact interface. However, Ge is an amphoteric dopant which produces heavily compensated material when high doping concentrations are attempted. The highest doping concentration reported for liquid-phase epitaxial growth of GaAs from Au-Ge<sup>8,9</sup> and Au-Ge-Ni<sup>9</sup> melts is about  $5 \times 10^{18}$  donors/cm<sup>3</sup>. For good ohmic behavior, as observed in these alloyed ohmic contacts, a doping density of at least  $5 \times 10^{19}$  donors/cm<sup>3</sup> is required.<sup>10</sup> Although bulk doping concentrations of this magnitude are not achievable, Kirchner *et al.*<sup>11</sup> claim, from specific contact resistivity measurements, that during molecular-beam epitaxial (MBE) growth a surface doping concentration of  $\sim 1 \times 10^{20}$  donors/cm<sup>3</sup> can be achieved (with Si). It may be argued that a similar phenomenon occurs in the Au-Ge-Ni contact, although there has not been any direct observation of this. The nonuniformity both laterally and in depth of these alloyed contacts makes such an observation particularly difficult. This nonuniformity can itself be a source of electron injection due to field emission.

In the case of the solid-phase contacts using Ge/Pd/GaAs, a significant increase in spatial uniformity is observed.<sup>12-15</sup> During ohmic contact formation some Ge is consumed in the formation of PdGe and excess Ge is transport-

ed to the GaAs surface where it grows epitaxially.<sup>12-15</sup> An alternative model for the ohmic behavior of this system is that the epitaxial Ge layer results in a low barrier contact to GaAs, as has been observed for MBE grown Ge/GaAs structures.<sup>16</sup> However, studies of ostensibly undoped Ge layers, of the temperature and doping dependence of the contact resistivity,<sup>13</sup> and of the increased contact resistance to *p*-type GaAs as compared with the pure Pd contact<sup>14</sup> are consistent with the doping model. It is suggested that Ge is incorporated into GaAs preferentially on Ga sites due to the formation of excess Ga vacancies<sup>15</sup> to yield an *n*<sup>+</sup> layer immediately beneath the contact. This paper sets out to resolve the extent of Ge incorporation which occurs, if at all, within nanometers of the contact interface.

Secondary ion mass spectrometry (SIMS) is an appropriate technique for this study since it possesses high depth resolution coupled with high (parts per million) sensitivity to the constituent elements, particularly Ge. The depth resolution of SIMS is dependent upon the sample roughness and nonuniformity,<sup>17</sup> ion beam mixing and knock-on effects,<sup>18,19</sup> preferential sputtering,<sup>19</sup> and segregation effects induced by oxygen bombardment.<sup>19,20</sup> These effects make it difficult to detect a thin layer of low concentration immediately beneath a layer of high concentration; in this case, a layer of Ge-doped GaAs beneath a Ge layer. In addition, polycrystalline metallic overlayers typically roughen considerably in the course of a sputter profile. To circumvent these difficulties, high depth resolution SIMS profiles were performed from the backside of chemically thinned samples, utilizing the technique developed by Palmström *et al.*,<sup>21</sup> described below.

Knowledge of sputter rate and depth resolution are essential when trying to extract quantitative information from SIMS depth profiles. Unfortunately, these parameters can vary from run to run and sample to sample. Here, internal marker layers of known thickness and spacing were incorpo-

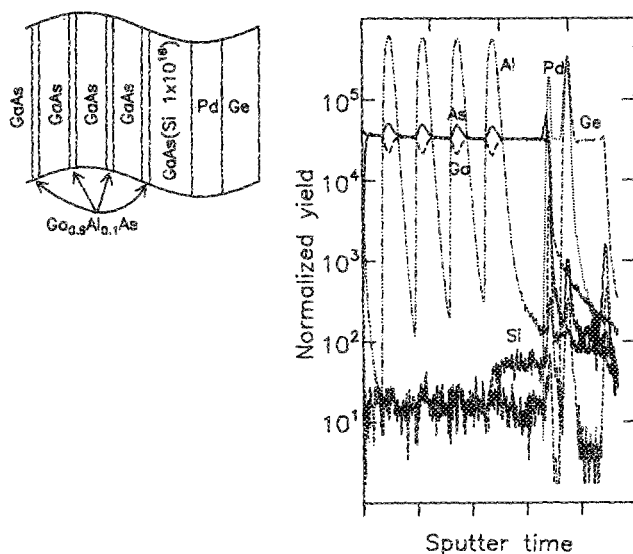


FIG. 1. Backside SIMS sputter depth profiles of an unannealed Ge/Pd/GaAs/ $4 \times [\text{Ga}_{0.9}\text{Al}_{0.1}\text{As}/\text{GaAs}]$  structure using 2.3 keV  $\text{O}_2^+$  ion beam.

rated in the samples in order to calibrate sputtering rate and depth resolution during each individual depth profile. The marker layers also allow for precise alignment of the depth profiles so that material consumption can be examined with a precision exceeding the inherent depth resolution of the technique. Molecular-beam epitaxy was used to grow the layer structures since this technique has great control of layer thickness, interface abruptness and layer composition. The marker layers were formed using four periods of GaAs(400 Å)/ $\text{Ga}_{0.9}\text{Al}_{0.1}\text{As}$ (100 Å) layers. These layers are atomically abrupt and the sputter rate is similar in GaAs and  $\text{Ga}_{0.9}\text{Al}_{0.1}\text{As}$ . The concentration of Al was chosen to minimize matrix effects but still give a substantial SIMS signal. An 800 Å Si-doped GaAs surface layer was also incorporated, permitting subsequent electrical measurements. In order to achieve maximum reproducibility, only samples fabricated from the same wafer will be directly compared.

A backside SIMS technique has been used previously to study the penetration depth of Au-Ge-Ni/GaAs alloyed contacts by Shappirio *et al.*<sup>22,23</sup> In their case alternating *n*-type and *p*-type GaAs layers were used as markers and the sample geometry was not designed to optimize depth resolution (roughly 3 μm of GaAs was sputtered before reaching the GaAs/contact interface).

## II. EXPERIMENT

The samples were grown by MBE in a Varian GenII MBE system. The following structure was grown by MBE on semi-insulating (Cr-doped) (100) GaAs: GaAs buffer (5000 Å)/AlAs (1000 Å)/ $4 \times [\text{GaAs}$  (400 Å)/ $\text{Ga}_{0.9}\text{Al}_{0.1}\text{As}$ (100 Å)]/GaAs(*n*-type Si-doped  $1 \times 10^{18} \text{ cm}^{-3}$ , 800 Å). The AlAs layer was used as a lift-off layer to enable removal of the substrate for backside SIMS. This technique for lifting off thin GaAs layers has been described recently.<sup>24</sup> Some samples had an additional  $\text{Ga}_{0.4}\text{Al}_{0.6}\text{As}$

layer 5000 Å thick grown between the AlAs and GaAs buffer layer. The MBE grown samples were degreased with TCE, ultrasonically cleaned with acetone and isopropanol, then rinsed in HCl:H<sub>2</sub>O (1:1 by volume) until hydrophobic, and finally rinsed in deionized H<sub>2</sub>O and blow dried in flowing N<sub>2</sub>. Immediately after drying, the samples were loaded into an ion pumped electron beam evaporator with a base pressure  $\sim 1.7 \times 10^{-8}$  Torr. Pd (470 Å) was deposited at 7 Å/s, followed by Ge (1500 Å) at 15 Å/s. The pressure during deposition was  $(1-3) \times 10^{-7}$  Torr. The samples were annealed in a forming gas ambient (15% H<sub>2</sub>-85% N<sub>2</sub>) at temperatures ranging from 325 to 410 °C. For electrical evaluation samples with transmission line (TLM) patterns were also fabricated simultaneously.

After annealing the metallization/GaAs/ $4 \times [\text{Ga}_{0.9}\text{Al}_{0.1}\text{As}(100 \text{ Å})/\text{GaAs}(400 \text{ Å})]$  structure was lifted off for backside SIMS analysis. The contact surface was protected using wax and the AlAs lift-off layer dissolved in an HF based etch.<sup>24</sup> The wax-supported structures were mounted contact side down in the SIMS instrument and depth profiles were performed from the semiconductor side of the samples. The samples with the additional  $\text{Ga}_{0.4}\text{Al}_{0.6}\text{As}$  layer were mounted contact side down on a GaAs substrate using wax. They were then thinned mechanically to  $\sim 50 \mu\text{m}$  before being etched in a H<sub>2</sub>O<sub>2</sub>-NH<sub>4</sub>OH etch. The  $\text{Ga}_{0.4}\text{Al}_{0.6}\text{As}$  layer acted as an etch stop layer enabling preferential removal of the substrate GaAs. The  $\text{Ga}_{0.4}\text{Al}_{0.6}\text{As}$  and AlAs were then removed using an HF based etch. Since two etch stop interfaces are employed, the resulting surface is near atomically smooth. SIMS measurements were performed in an Atomica 3000-30 ion microprobe utilizing a 2.3 or 6.6 keV  $\text{O}_2^+$  ion beam at normal incidence. A Ge implanted GaAs standard was used for calibration. RBS measurements were performed using a 3 MeV He<sup>++</sup> ion beam produced by a General Ionex 1-MV Tandatron accelerator. The transmission line method (TLM) was used to determine the specific contact resistance of the ohmic contacts.

## III. RESULTS

Figure 1 shows a backside SIMS depth profile of an unannealed Ge/Pd/GaAs structure. Note that the front edge of each Al peak is sharper than the back due to ion beam mixing (knock on).<sup>18</sup> Since the GaAs/ $\text{Ga}_{0.9}\text{Al}_{0.1}\text{As}$  interfaces grown by MBE may be assumed to be atomically abrupt, the transition width of this front edge is a measure of the depth resolution during each depth profile. The peak-to-valley ratio for the Al signal in Fig. 1 decreases with sputter depth, indicating a slight decrease in depth resolution with sputtering. For the Al layer closest to the contact the 10%-90% widths of the front and back edges were  $\sim 50$  and  $\sim 85$  Å, respectively. In determining low concentrations close to an interface the signal rise and decay rates are also important. For the  $\text{Ga}_{0.9}\text{Al}_{0.1}\text{As}$  layer closest to the contact the Al signal rise rate was determined to be  $\sim 10 \text{ Å/decade}$  at the GaAs/ $\text{Ga}_{0.9}\text{Al}_{0.1}\text{As}$  interface and the decay rate to be  $\sim 90 \text{ Å/decade}$  at the  $\text{Ga}_{0.9}\text{Al}_{0.1}\text{As}/\text{GaAs}$  interface using a 2.3 keV  $\text{O}_2^+$  beam. The small signals of Ge and Pd in the semiconductor layers arise from background noise in the SIMS

instrument. When the GaAs/contact interface is reached, the Pd signal can be seen to rise much faster than the Ge signal (20 Å/decade vs 50 Å/decade). This shows that Pd is in contact with GaAs. The Pd signal then drops before it rises again at the Pd/Ge interface. The Ga and As signals are also observed to increase at the GaAs/Pd interface. The rate of rise for the Pd signal indicates that this interface is abrupt.

Figure 2 shows the GaAs/Pd/Ge interface more clearly. A 6.6 keV  $O_2^+$  ion beam was used in this case. Figure 2(a) shows the frontside profile (i.e., from the contact surface) and Fig. 2(b) the backside. The horizontal axis (sputter time) has been normalized such that the sputter rate for GaAs is the same in each case. It can easily be seen that the depth resolution at the GaAs/Pd interface has been substantially improved by backside SIMS. A Pd signal rise rate of  $\sim 30$  Å/decade was determined for Fig. 2(b) and Pd signal decay rate of  $\sim 250$  Å/decade for Fig. 2(a).

Figure 3 shows RBS backscattering spectra of the Ge/Pd/GaAs structure after various anneals. The as-deposited spectrum shows the Ge/Pd/GaAs structure. Annealing at 225 °C results in PdGe formation at the Ge/Pd interface. However, some unreacted Ge remains at the surface as can be inferred from the Ge peak at the surface and the high-energy edge of the Pd peak which has not reached its surface value. Annealing at 325 °C results in Ge accumulation at the GaAs surface with no elemental Ge remaining on the contact surface. The associated SIMS depth profiles are shown in Fig. 4. The unannealed sample shows an abrupt GaAs/Pd interface [Fig. 4(a)] with a 20 Å/decade rise rate of the Pd signal. There is no Ge detected in the as-deposited Pd film. The SIMS depth profile for the 225 °C annealed sample [Fig. 4(b)] shows that Pd and Ge have reacted. The Ga and As signals show peaks at the interface as in the unannealed sample. Annealing at 325 °C results in these peaks disappearing when Ge comes into contact with GaAs [Fig. 4(c)]. There is little Pd in the interfacial Ge layer. These results are consistent with the RBS data shown in Fig. 3.

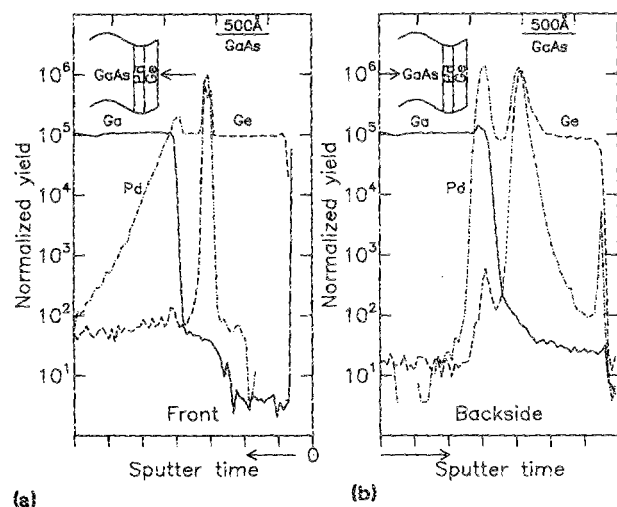


FIG. 2. SIMS profiles of an unannealed Ge/Pd/GaAs structure using 6.6 keV  $O_2^+$  ion beam: (a) from the front and (b) from the back. The depth scale marker is for the GaAs only.

The amount of GaAs consumption during ohmic contact formation can be determined from Fig. 5. Here the marker layers allow precise alignment of unannealed and annealed profiles. The shift in interface position corresponds to a  $\sim 40$  Å consumption of GaAs. This is  $\leq 5\%$  of the 800 Å GaAs surface layer thickness and within the experimental tolerance.

SIMS profiles were also obtained from samples which underwent a second anneal, as shown in Fig. 6. The SIMS depth profile for a 225 °C, 30 min/325 °C, 30 min dual anneal [Fig. 6(a)] is virtually identical to the profile of the 325 °C, 30 min annealed sample [Fig. 4(c)]. Figure 6(b) shows the SIMS depth profile of a 325 °C, 30 min/410 °C, 1 h annealed sample. Again, the profile is very similar to that for the 325 °C annealed sample except that significant penetration of Ge (of the order of 200 Å) into the GaAs is observed.

The TLM measurements of these contacts showed that the as-deposited samples were rectifying, the 225 °C annealed sample was a poor ohmic contact ( $r_c \sim 1 \times 10^{-3} \Omega \text{ cm}^2$ ) while the 325 °C sample showed good ohmic behavior ( $r_c \sim 1.4 \times 10^{-6} \Omega \text{ cm}^2$ ). The dual anneal at 225 °C/325 °C yielded virtually identical contact resistivity to the sample annealed at 325 °C only. The 325 °C/410 °C dual anneal showed an increase in the specific contact resistance ( $r_c \sim 5 \times 10^{-6} \Omega \text{ cm}^2$ ).

## IV. DISCUSSION

### A. Comparisons

The backscattering results in Fig. 3 and the SIMS results in Fig. 4 are consistent and in complete agreement with earlier published results on the Ge/Pd/GaAs contacts.<sup>12-15</sup> It has been shown with transmission electron microscopy that

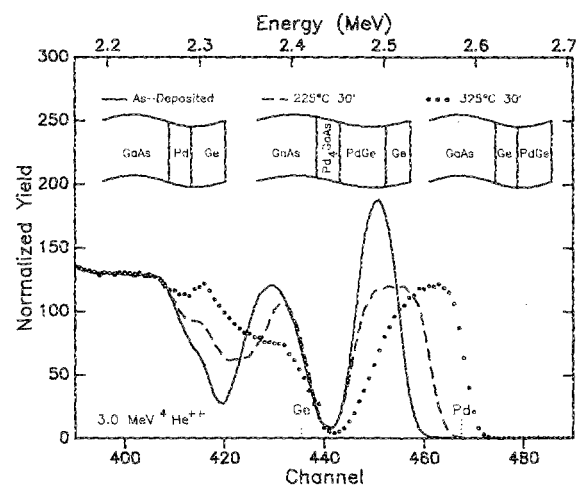


FIG. 3. Backscattering spectra of Ge/Pd/GaAs/ $4 \times [Ga_{0.9}Al_{0.1}As/GaAs]/AlAs/Ga_{0.4}Al_{0.6}As/GaAs$  unannealed and annealed 225 °C, 30 min and 325 °C, 30 min.

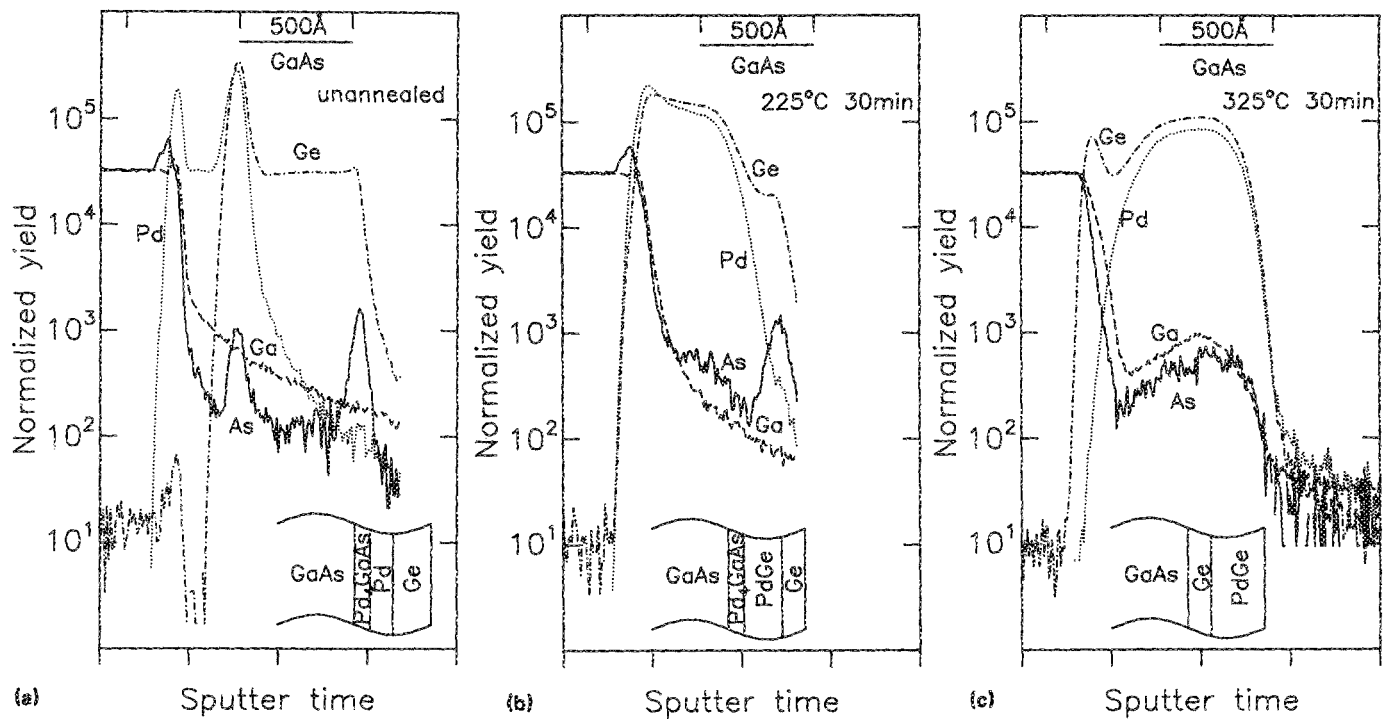


FIG. 4. Backside SIMS sputter depth profiles of unannealed and annealed Ge/Pd/GaAs structures using 2.3 keV  $O_2^+$  ion beam: (a) unannealed; (b) 225 °C, 30 min; and (c) 325 °C, 30 min. The depth scale marker is for the GaAs only.

Pd reacts with GaAs during deposition to form a thin interfacial layer ( $\sim 60$ – $120$  Å) of  $Pd_4GaAs$ .<sup>25</sup> The presence of the  $Pd_4GaAs$  layer has also been observed by x-ray diffraction.<sup>26</sup> This layer was found to be present in samples as-deposited and annealed at 225 °C, but was not detected in contacts annealed at 250 °C and above.<sup>26</sup> The backscattering results in Fig. 3 cannot detect this layer due to lack of resolution. The rise in the Ga and As SIMS signals at the GaAs/Pd interface [Fig. 4(a)] is interpreted as a signature of

$Pd_4GaAs$  formation at the interface. Similarly, the large rise in the Ge signal at the Pd/Ge interface may also be indicative of a Pd-Ge reaction during deposition. Clearly, there is no significant Pd indiffusion into the GaAs beneath this reacted layer; the as-deposited structure consists of GaAs/ $Pd_4GaAs$ /Pd/Ge.

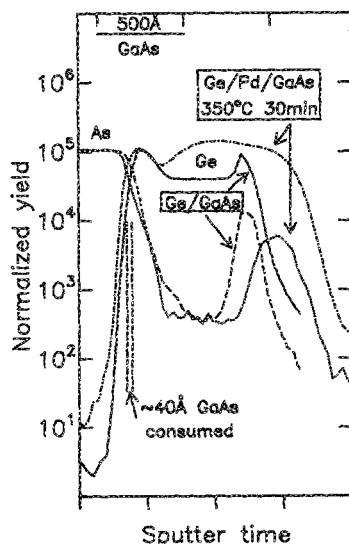


FIG. 5. Backside SIMS sputter depth profiles of unannealed Ge/GaAs and annealed 350 °C, 30 min Ge/Pd/GaAs structures using 6.6 keV  $O_2^+$  ion beam. The depth scale marker is for the GaAs only.

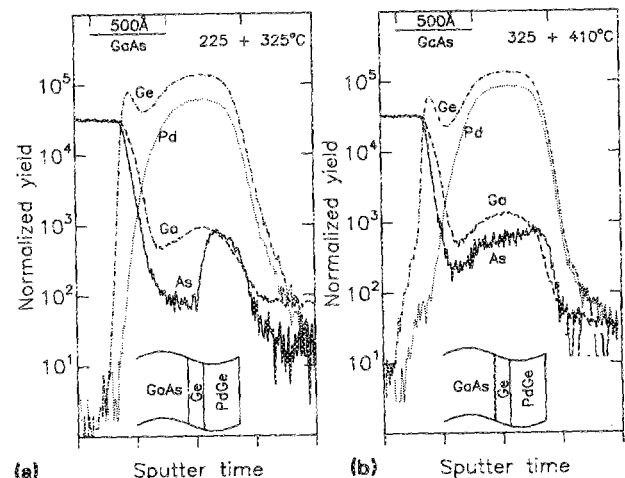


FIG. 6. Backside SIMS sputter depth profiles of double annealed Ge/Pd/GaAs structures using 2.3 keV  $O_2^+$  ion beam: (a) 225 °C, 30 min + 325 °C, 30 min; and (b) 325 °C, 30 min + 410 °C, 1 h. The depth scale marker is for the GaAs only.

Annealing at 225 °C results in a Pd-Ge reaction with the formation of PdGe, as inferred from Figs. 3 and 4(b). Both backscattering and SIMS show that there is little transport of Ge from the contact surface through the PdGe to the GaAs surface. However, SIMS does show a presence of Ge at the GaAs surface [Fig. 4(b)]. The SIMS results in Fig. 4(b) show the Ga and As signal rise at the GaAs/Pd interface, which is indicative of a Pd<sub>4</sub>GaAs layer. Furthermore, the Pd signal can be seen to rise more rapidly at high signal level than the Ge, consistent with the presence of a thin layer richer in Pd than Ge. Hence, it can be concluded that the Pd<sub>4</sub>GaAs layer is still present. The contact structure has become GaAs/Pd<sub>4</sub>GaAs(Ge)/PdGe/Ge. The presence of some Ge in the GaAs interface region may explain the change in the electrical properties of the contact in going from rectifying to poor ohmic.

It can be deduced from both the backscattering (Fig. 3) and SIMS [Fig. 4(c)] results that annealing at 325 °C results in Ge accumulation at the GaAs/contact interface. Again this is in agreement with earlier studies.<sup>12-15</sup> These results cannot determine whether this arose from Ge transport through the PdGe and/or Pd out-diffusion. The lack of Pd at the GaAs surface and Ga/As yield increase at the GaAs/Ge interface shows that the interfacial Pd<sub>4</sub>GaAs layer no longer exists in agreement with x-ray diffraction studies.<sup>26</sup>

## B. Regrowth, dissolution, and doping

If a thin highly doped GaAs layer is formed during ohmic contact formation, then this could occur either through diffusion of Ge into the GaAs or by solid phase regrowth of GaAs doped with Ge. Solid phase regrowth of GaAs from Ni<sub>3</sub>GaAs has been shown to occur in Si/Ni/GaAs structures.<sup>27</sup> It is important to determine whether a similar mechanism is occurring in Ge/Pd/GaAs contacts. During the deposition of Pd on GaAs, a thin layer (60–120 Å) of Pd<sub>4</sub>GaAs phase forms.<sup>25</sup> According to Sands *et al.*,<sup>25</sup> this phase can grow to a maximum thickness of ~250 Å at 275 °C before the next ternary phase starts to grow. They found that the second phase did not form at temperatures below 250 °C. A similar amount of Pd<sub>4</sub>GaAs formation was reported by Lin *et al.* for a 250 °C, 1 h anneal<sup>28</sup> (150 Å of Pd was consumed by reaction, which corresponds to ~225 Å Pd<sub>4</sub>GaAs). The formation of 60–250 Å Pd<sub>4</sub>GaAs would result in the consumption of ~30–130 Å of GaAs. From Fig. 5 it was deduced that ~40 Å of GaAs is consumed during contact formation, which is in the range of that predicted from Pd<sub>4</sub>GaAs formation. The error in consumed GaAs is estimated to be ±20 Å due to sample nonuniformity and beam current drift.

In comparing Figs. 4(b) and 4(c) it is clear that the Ga yield in the contact metallization has increased by about one order of magnitude and is about two orders of magnitude lower than in GaAs. 50 Å of GaAs corresponds to ~1×10<sup>16</sup> Ga atoms/cm<sup>2</sup>. The contact metallization consisted of 470 Å Pd and 1500 Å Ge, which corresponds to ~1×10<sup>18</sup> atoms/cm<sup>2</sup>. Thus, if all the Ga in the Pd<sub>4</sub>GaAs layer were dispersed in the contact metallization uniformly it would be present at a level ~1 at. %, which is probably below the

solubility limit. The Ga and As are uniformly distributed so that there is no diffusion limitation to the dissolution of GaAs. Assuming that the Ga ionization yield is similar in PdGe and GaAs the Ga yield in the PdGe would, in fact, correspond to about 1 at. %. In short, consumption and dissolution of GaAs clearly occurs, but the extent of GaAs regrowth, which depends on the Pd<sub>4</sub>GaAs thickness, cannot be accurately determined; it is anticipated to be between 0 and 50 Å. Lattice imaging of an annealed ohmic sample in the presumably analogous Si/Pd/GaAs system has shown evidence for a regrown GaAs layer on the order of 100 Å thick.<sup>15</sup>

The rate of Ge signal rise at the GaAs/Ge interface was ~20 Å/decade, which is comparable to the as-deposited GaAs/Pd interface and only slightly worse than the GaAs/Ga<sub>0.9</sub>Al<sub>0.1</sub>As interface (~10 Å/decade). Hence, the amount of Ge in-diffusion into the GaAs must also be small. The data cannot rule out the formation of an extremely thin Ge-doped GaAs layer. From a Ge-implanted GaAs standard, a normalized ion yield of 50 in Fig. 4 corresponds to 1×10<sup>19</sup> Ge atoms/cm<sup>3</sup>. This level occurs at a depth of ~90 Å beneath the interface. Thus the maximum thickness for a Ge-doped GaAs layer with Ge doping ≥1×10<sup>19</sup> cm<sup>-3</sup> is ~90 Å. This number may be dominated by instrumental broadening and interface roughness. The *n*<sup>+</sup>-GaAs regrowth model requires that a layer of doping 10<sup>20</sup> cm<sup>-3</sup> be at least 30 Å in thickness to yield ohmic behavior.

Degradation in contact resistance after annealing at 410 °C correlates with Ge diffusion into the GaAs. This might be expected since high doping concentrations of Ge in GaAs results in highly compensated material and in some cases even *p*-type material. However, under ideal conditions, *n*<sup>+</sup> doping levels ~7×10<sup>19</sup>/cm<sup>3</sup> have been achieved.<sup>29</sup>

## C. Alternative models

In determining the formation of a thin Ge doped GaAs layer, it has been assumed that the doping levels of interest are in the range of 1×10<sup>19</sup>–1×10<sup>20</sup>/cm<sup>3</sup>. Another mechanism which may also be the cause of ohmic behavior is the formation of a thin ternary Ge<sub>x</sub>(GaAs)<sub>1-x</sub> (Ref. 30) layer with a small band gap between the regrown Ge and GaAs. Ion beam mixing and variations in ion yields at high concentrations makes this difficult to detect using SIMS alone.

The presence of Ge at the contact/GaAs interface is observed by SIMS in samples annealed at temperatures as low as 225 °C [Fig. 4(b)]. The interfacial Ge could be contained in a Ge/GaAs heterojunction, the Pd<sub>4</sub>GaAs layer or in PdGe which is in contact with the GaAs as a result of nonuniform decomposition of Pd<sub>4</sub>GaAs. A Ge/GaAs heterojunction may exhibit ohmic behavior,<sup>16</sup> in which case the doping of the Ge becomes an issue. As yet the doping level and type in the Ge layers formed in these Ge/Pd/GaAs contacts has not been determined. Recent low-temperature electrical measurements suggest that an effective barrier of ~0.01–0.02 eV is present in this contact.<sup>31</sup> This is only slightly lower than the conduction band discontinuity for an MBE *n*<sup>+</sup>-Ge/*n*<sup>-</sup>-GaAs heterojunction (~0.08 eV).<sup>32</sup> A lower effective barrier height might be expected for *n*<sup>+</sup>-

Ge/ $n^+$ -GaAs. However, if the mechanism for the ohmic behavior in the Si/Pd/GaAs and Ge/Pd/GaAs systems are the same, then the  $n^+$ -Ge/ $n^+$ -GaAs heterojunction is unlikely to be responsible for the ohmic behavior since no Si/GaAs heterojunction has been observed. On the other hand, preliminary SIMS results indicate no significant in-diffusion of Si also in the Si/Pd/GaAs system.

For ohmic behavior to be observed, changes in the GaAs surface region have to occur to enable easy carrier transport across the Ge/GaAs interface. Either an  $n^+$ -GaAs surface layer is formed, the Fermi-level pinning position for the GaAs surface is modified to give a low barrier at the Ge/GaAs interface [such as may happen if a thin  $\text{Ge}_x(\text{GaAs})_{1-x}$  were formed between the Ge and GaAs], or a defective regrown GaAs surface layer is present.<sup>33</sup> The electrical data for these contacts on  $p$ -type GaAs, which show poor ohmic or rectifying behavior,<sup>34</sup> are not inconsistent with  $n^+$ -regrown GaAs layer or a  $n^+$ -Ge/ $n^+$ -GaAs heterojunction model. These data could also be explained by a lowered effective barrier height to  $n$ -type GaAs by the formation of a thin  $\text{Ge}_x(\text{GaAs})_{1-x}$  intermediate layer, Fermi-level unpinning at the GaAs surface, or movement to another pinning position.

## V. CONCLUSIONS

Backside SIMS can be used to study doping level concentrations of overlayer impurities immediately beneath an interface. This enables direct detection of in-diffusion into the underlayer. SIMS signal rise rates of 20 Å/decade have been demonstrated for GaAs/metallization interfaces.

The onset of ohmic behavior in the Ge/Pd/GaAs system is found to occur when Ge is detected at the GaAs surface. Good ohmic behavior is observed when an interfacial layer of reacted  $\text{Pd}_4\text{GaAs}$  is dispersed and complete coverage of Ge occurs. Degradation in the ohmic behavior correlates with Ge diffusion into the GaAs beneath the contact. This ohmic contact is extremely shallow; after contact formation only  $\sim 40$  Å GaAs is consumed and the maximum Ge penetration depth is less than 100 Å.

These results place strict limitations on the models for ohmic contact formation. Significant consumption and dissolution of GaAs occurs in the contact, limiting the amount of GaAs available for regrowth. For the  $n^+$ -GaAs regrown layer model, the thickness of any regrown GaAs layer and the extent of Ge in-diffusion must be significantly less than 100 Å immediately beneath the contact.

## ACKNOWLEDGMENTS

The authors would like to acknowledge R. J. M. Griffiths for information on preferential etching procedures and J. Conner and L. Nazar for assistance in sample preparation. Discussions with T. Sands are much appreciated. UCSD acknowledges support from Defense Advanced Research Proj-

ect Agency (DARPA) Contract [No. MDA-903-87-K-0762 P00004] (A. Prabhakar and S. Roosild).

- <sup>1</sup>C. J. Palmström and D. V. Morgan, in *Gallium Arsenide: Materials, Devices, and Circuits*, edited by M. J. Howes and D. V. Morgan, (Wiley, New York, 1985), p. 195.
- <sup>2</sup>B. L. Sharma, in *Semiconductors and Semimetals* (Academic, New York, 1981), Vol. 15, p. 1.
- <sup>3</sup>V. L. Rideout, *Solid-State Electron.* **18**, 541 (1975).
- <sup>4</sup>M. N. Yoder, *Solid-State Electron.* **23**, 117 (1980).
- <sup>5</sup>A. Piotrowska, A. Guivarc'h, and G. Pelous, *Solid-State Electron.* **26**, 179 (1983).
- <sup>6</sup>N. Braslau, *Thin Solid Films* **104**, 391 (1983).
- <sup>7</sup>N. Braslau, J.B. Gunn, and J.L. Staples, *Solid-State Electron.* **10**, 381 (1967).
- <sup>8</sup>A. M. Andrews and N. Holonyak, Jr., *Solid-State Electron.* **15**, 601 (1972).
- <sup>9</sup>M. Otsubo, H. Kumabe, and H. Miki, *Solid-State Electron.* **20**, 617 (1977).
- <sup>10</sup>W. J. Devlin, C. E. C. Wood, R. Stall, and L. F. Eastman, *Solid-State Electron.* **23**, 823 (1980).
- <sup>11</sup>P. D. Kirchner, T. N. Jackson, G. D. Pettit, and J. M. Woodall, *Appl. Phys. Lett.* **47**, 26 (1985).
- <sup>12</sup>E. D. Marshall, C. S. Wu, D. M. Scott, S. S. Lau, and T. F. Kuech, *Mater. Res. Symp. Proc.* **25**, 63 (1984).
- <sup>13</sup>E. D. Marshall, W. X. Chen, C. S. Wu, S. S. Lau, and T. F. Kuech, *Appl. Phys. Lett.* **47**, 298 (1985).
- <sup>14</sup>E. D. Marshall, B. Zhang, L. C. Wang, P. F. Jiao, W. X. Chen, T. Sawada, S. S. Lau, K. L. Kavanagh, and T. F. Kuech, *J. Appl. Phys.* **62**, 942 (1987).
- <sup>15</sup>L. C. Wang, B. Zhang, F. Fang, E. D. Marshall, S. S. Lau, T. Sands, and T. F. Kuech, *J. Mater. Res.* **3**, 922 (1988).
- <sup>16</sup>R. Stall, C. E. C. Wood, K. Board, N. Dandekar, L. F. Eastman, and J. Devlin, *J. Appl. Phys.* **52**, 4062 (1981).
- <sup>17</sup>D. S. McPhail, E. A. Clark, M. G. Dowsett, H. S. Fox, and A. Lovejoy, in *Secondary Ion Mass Spectrometry SIMS VI*, edited by A. Benninghoven, A. M. Huber, and H. W. Werner (Wiley, New York, 1988), p. 495.
- <sup>18</sup>S. A. Schwarz and C. R. Helms, *J. Vac. Sci. Technol.* **16**, 781 (1979).
- <sup>19</sup>K. Wittmaack, *Vacuum* **34**, 119 (1984).
- <sup>20</sup>S. D. Littlewood, J. A. Kilner, and J. P. Gold, in *Secondary Ion Mass Spectrometry SIMS VI*, edited by A. Benninghoven, A. M. Huber, and H. W. Werner (Wiley, New York, 1988), p. 737.
- <sup>21</sup>C. J. Palmström, S. A. Schwarz, E. D. Marshall, E. Yablonovitch, J. P. Harbison, C. L. Schwartz, L. Florez, T. J. Gmitter, L. C. Wang, and S. S. Lau, *Mater. Res. Symp. Proc.* **126**, 283 (1988).
- <sup>22</sup>J. R. Shappiro, R. T. Lareau, R. A. Lux, J. J. Finnegan, D. D. Smith, L. S. Heath, and M. Taysing-Lara, *J. Vac. Sci. Technol. A* **5**, 1503 (1987).
- <sup>23</sup>R. T. Lareau, in *Secondary Ion Mass Spectrometry SIMS VI*, edited by A. Benninghoven, A. M. Huber, and H. W. Werner (Wiley, New York, 1988), p. 437.
- <sup>24</sup>E. Yablonovitch, T. Gmitter, J. P. Harbison, and R. Bhat, *Appl. Phys. Lett.* **51**, 2222 (1987).
- <sup>25</sup>T. Sands, V. G. Keramidas, A. J. Yu, K.-M. Yu, R. Gronsky, and J. Washburn, *J. Mater. Res.* **2**, 262 (1987).
- <sup>26</sup>E. D. Marshall, L. S. Yu, S. S. Lau, and T. F. Kuech, paper presented at the EMC meeting, Boulder, Colorado, June 22–24, 1988.
- <sup>27</sup>T. Sands, E. D. Marshall, and L. C. Wang, *J. Mater. Res.* **3**, 915 (1988).
- <sup>28</sup>J.-C. Lin, K.-C. Hsieh, K. J. Schulz, and Y. A. Chang, *J. Mater. Res.* **3**, 148 (1988).
- <sup>29</sup>R. Stall, Ph.D. thesis, Cornell University, 1981.
- <sup>30</sup>S. A. Barnett, M. A. Ray, A. Lastras, B. Kramer, J. E. Greene, P. M. Raccach, and L. L. Abels, *Electron. Lett.* **18**, 891 (1982).
- <sup>31</sup>L. S. Yu, L. C. Wang, E. D. Marshall, S. S. Lau, and T. F. Kuech, *J. Appl. Phys.* **65**, 1621 (1989).
- <sup>32</sup>J. M. Ballingall, C. E. C. Wood, and L. F. Eastman, *J. Vac. Sci. Technol. B* **1**, 675 (1983).
- <sup>33</sup>T. Sebestyen, *Solid State Electron.* **25**, 543 (1982).
- <sup>34</sup>E. D. Marshall (unpublished).